

phys. stat. sol. (a) **180**, 327 (2000)

Subject classification: 73.61.Ey; 78.47.+p; 78.55.Cr; 78.60.Hk; S7.14

Comparison of the Mechanism of Optical Amplification in InGaN/GaN Heterostructures Grown by Molecular Beam Epitaxy and MOCVD

J. HOLST (a), A. KASCHNER (a), U. GFUG (a), A. HOFFMANN (a), C. THOMSEN (a), F. BERTRAM (a), T. RIEMANN (b), D. RUDLOFF (b), P. FISCHER (b), J. CHRISTEN (b), R. AVERBECK (c), H. RIECHERT (c), M. HEUKEN (d), M. SCHWAMBERA (d), and O. SCHÖN (d)

(a) *Institut für Festkörperphysik, TU Berlin, Hardenbergstraße 36, D-10623 Berlin, Germany*

(b) *Institut für Experimentelle Physik, Otto-von-Guericke-Universität, PO Box 4120, D-39016 Magdeburg, Germany*

(c) *Infineon Technologies AG, Corporate Research, CPR 7, D-81730 München, Germany*

(d) *AIXTRON AG, Kackerstraße 15–17, D-52072 Aachen, Germany*

(Received March 6, 2000)

We comprehensively studied InGaN/GaN heterostructures grown by molecular beam epitaxy (MBE) and metal-organic vapor deposition epitaxy (MOCVD) using a variety of methods of optical spectroscopy, such as cathodoluminescence microscopy (CL), time-integrated and time-resolved photoluminescence (PL). Micro-photoluminescence and cathodoluminescence results show the variation in emission wavelength at different scales, and this reflects the degree of compositional fluctuations in the samples. We obtain information on the decay times of the main emission lines using time-resolved photoluminescence spectroscopy and models of stretched exponentials, indicating the importance of nanoscale fluctuations for the recombination mechanism. The temperature dependent behavior of the InGaN emission is explained in terms of a carrier freeze out at local potential fluctuations combined with a thermionic thermalization at elevated temperatures. To correlate the fluctuations in emission wavelength with values for the optical amplification we performed gain measurements in edge-stripe geometry. From all these results we conclude, that localized carriers at a statistical distribution of potential fluctuations act as recombination centers and that the degree of fluctuations determines the efficiency of optical amplification. The threshold values for lasing and the gain values are compared and discussed with respect to the different growth procedures. From all these findings we draw conclusions concerning the influence of differences in the growth conditions and their impact on the optical properties.

Introduction Heterostructures of compound group-III nitride semiconductors are of great importance for the rapidly increasing market of optoelectronic devices in the blue spectral range [1]. While most articles in this field report on investigation of samples grown by metal-organic vapor phase techniques [2 to 4] we expand our focus on InGaN grown by MBE to gain a deeper understanding of the fundamental recombination processes in h-InGaN heterostructures. The most reliable devices used for LEDs or LDs are produced by MOCVD. This is interesting because one would expect a better device performance by quasi-homoepitaxially grown MBE heterostructures. Therefore, it is the first aim of this paper to report on studies of the recombination mechanism

and the gain processes in InGaN heterostructures and to compare the results with respect to the different growth regimes, MBE and MOCVD. It is known that fluctuations in indium concentration as well as the miscibility gap [5], are major issues concerning the optical properties of the InGaN alloy system. Recently, the formation of InN quantum dots [6], potential fluctuations [7] or the quantum-confined Stark effect due to piezoelectric fields [8] were suggested to be the origin of the luminescence in the material. Thus, another focus of this paper will be to investigate the impact of the degree of In fluctuations on the optical amplification and from that to draw conclusions on the influence of the different growth processes.

Experimental Details Time-integrated photoluminescence experiments at different temperatures were performed using the 325 nm line of a He–Cd Laser. For time-resolved measurements a single photon counting setup was used with a 50 ps FWHM response to the laser pulse. A frequency-doubled Ti:sapphire laser was used for excitation at a wavelength of 370 nm, i.e. above the GaN band gap. The photoluminescence signal was analyzed in a 0.35 m subtractive double spectrometer and detected by a microchannel plate photomultiplier. The setup for the CL microscopy experiments is described in Ref. [9]. For the time-integrated high-excitation investigations we used a dye laser pumped by an excimer laser, providing pulses with a duration of 15 ns at a rate of 30 Hz and a total energy of up to 20 μ J at 340 nm. The samples were mounted in a bath cryostat at 1.8 K. Gain measurements were performed using the variable-stripe-length method [10].

Sample A belongs to a series of MBE-grown samples on sapphire, with an 18 μ m GaN (MOVPE) layer and capped by a 30 nm GaN layer. Sample A is a 10 \times 5 nm InGaN multiple-quantum well (MQW) with 4 nm GaN barriers with an indium concentration of 6.7%, as determined by XRD. Sample B is also a 10-fold InGaN/GaN multiple quantum well structure with a thickness of 4 nm each, grown with different growth temperatures for the quantum wells and barriers by low pressure MOCVD on \approx 2 μ m GaN/c-Al₂O₃ substrates in a horizontal production-type reactor AIX 2600 G3 in 2000 HT configuration. The In-composition was measured by XRD to be 12.5% with a GaN barrier thickness of 7.7 nm. The GaN buffer layer was grown at 1180 $^{\circ}$ C with hydrogen as the carrier gas at 200 mbar total pressure. The growth temperature of the InGaN quantum wells and the GaN barriers was 750 and 950 $^{\circ}$ C, respectively. Details are described in [11]. For comparison of the results of the MBE growth we will mention another sample C, which consists of 120 nm thick InGaN layer with an In content of 21%, but is not grown on a MOVPE-GaN template.

Results Figure 1 shows the temperature dependence of the luminescence spectra of samples A and B. One can distinguish two different PL peaks of sample A, which change their relative intensities with temperature. At very low temperatures (10 to 70 K) and at room temperature the high-energy peak dominates the spectra. For both samples the luminescence exhibits an “S-shaped” emission position shift with temperature as can be seen in the insets of Fig. 1. This behavior (redshift–blueshift–redshift) was first explained by Cho et al. [12] in terms of inhomogeneity and carrier localization in the InGaN. In this interpretation the high-energy peak is not only one emission line, but the spatially integrated luminescence of locally different recombination energies, which mirrors the distribution of potential fluctuations. With increasing temperature the

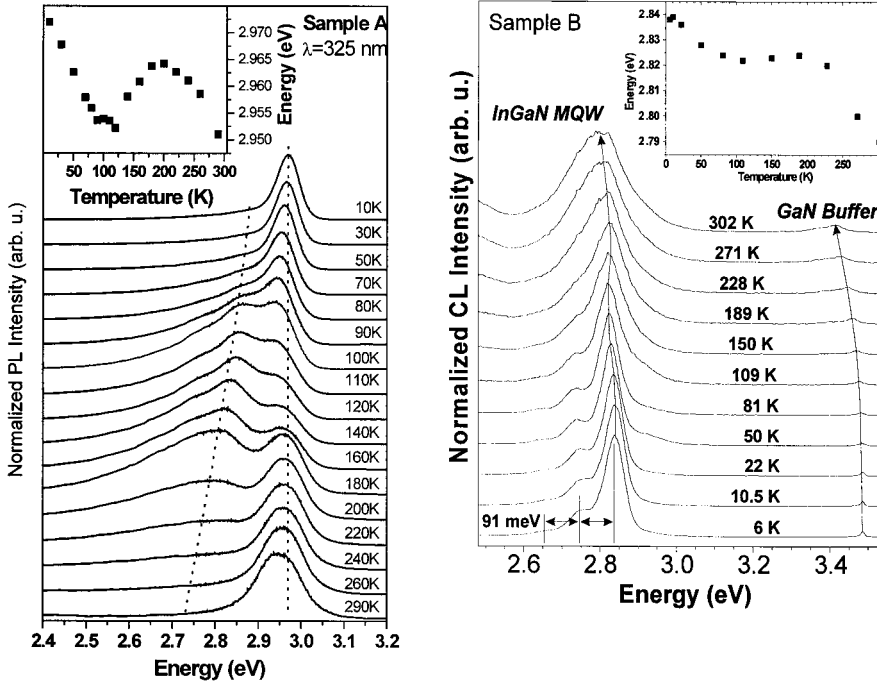


Fig. 1. Temperature dependent PL/CL of the InGaN MQW samples A (left) and B (right) at low excitation. Inset: S-shape of peak position versus temperature

localized carriers are frozen at the potential fluctuations leading to the observed blue-shift of peak position and thermalize at elevated temperatures.

We assign the low-energy peak in sample A being dominant between 90 and 180 K as recombination from electronic states deeper in the band gap. The “S-shape” behavior becomes less pronounced with increasing excitation power as was shown for both samples. This can also be understood in terms of band filling of localized states of InGaN [13]. It should be noticed that this temperature dependent behavior cannot be explained in terms of a quantum-confined Stark effect.

With increasing excitation density a strong shift of the peak position to higher energies is observed. This is depicted in Fig. 2. The excitation density was varied over seven orders of magnitude, resulting in a blueshift of about 180 meV. The energy shift obeys the expression

$$E_{\text{peak}}(I_{\text{exc}}) = E_0 + 25 \text{ meV} \log(I/I_0)$$

indicating the filling of localized states within a statistical In fluctuation with increasing excitation density. This behavior can also be interpreted in terms of screening piezoelectric fields, which are present in the samples. All these results are consistent in both samples and we can state that the recombination mechanism is similar in MOCVD- and MBE-grown InGaN heterostructures. This is confirmed by time-resolved PL experiments in which a multiple exponential decay for all spectral positions and for all samples was investigated. The dynamic behavior can be described by $\exp[-(t/\tau)\beta]$, the so-

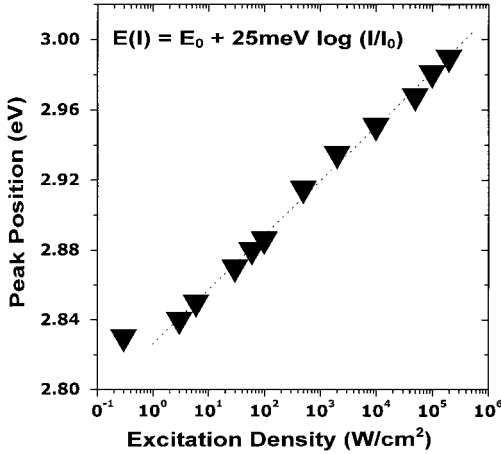


Fig. 2. Intensity dependent PL peak position of sample B by variation of excitation density by seven orders of magnitude

called stretched exponential. Our results for the luminescence decay indicate that the samples under investigation are disordered and that localized states contribute to the radiative recombination. We believe that the disorder arises from local potential fluctuations which can be due to thickness variations of the quantum wells or In composition fluctuations [14].

To achieve more information about the potential fluctuations we use the re-

sults of the CL measurements. We attribute the differences in the wavelength images of the samples to potential fluctuations, originating mainly from In-composition fluctuations. HRXRD measurements revealed very smooth quantum wells, excluding a strong influence of potential fluctuations from thickness variations. Table 1 summarizes the histograms of the samples, i.e. the number of occurrence of an emission energy in the CL wavelength image of a certain area. For samples A and B we find relatively narrow Gaussian distributions, whereas for the sample C the histogram is much broader and non-Gaussian. A Gaussian distribution indicates that the emission energies are random distributed on a lateral scale much smaller than the spatial resolution of the CL measurements (45 nm). For sample C the fluctuations are on a much larger scale, i.e. in the order of the spatial resolution or above. The difference between sample C and the others cannot be explained by the higher indium content, since alloy broadening following $[x(1-x)]^{1/2}$ cannot explain the much broader distribution with a change in line shape. For the MBE-grown samples it was evidenced that the improvement of adjusted growth conditions and the use of the MOVPE-GaN templates are the reasons for the lower In fluctuation in sample A compared to sample C. From the experimental results we conclude that the main recombination mechanism is due to localized carriers at potential fluctuations, which result mostly from In composition fluctuations. This indicates the strong impact of the degree of In fluctuations on the optical properties.

But what is the impact of these In fluctuations on the efficiency of optical amplification? Figure 3 shows the optical gain and lasing of samples A and B as function of energy in comparison to low excitation conditions. From site-selective PL excitation spectroscopy

Table 1

sample	Gaussian fit of CL histograms		E_{gain} (eV) at 7 K	max. gain (cm ⁻¹) at 6 K, 2 MW/cm ²
	E_{center} (eV)	σ		
A (MBE)	3.171	0.011265	3.213	62
B (MOCVD)	2.838	0.007095	3.00	130
C (MBE)	2.561	0.0805	—	—

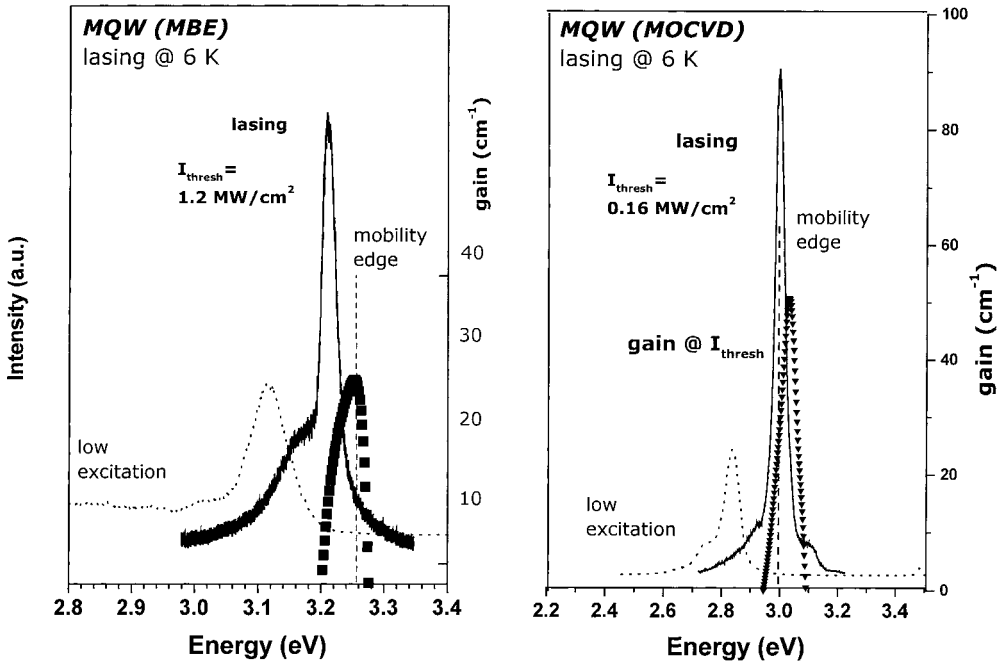


Fig. 3. Lasing (solid line) and gain spectra (squares/triangles) of the MBE-grown sample A (left) and the MOCVD-grown sample B (right) at 6 K in comparison to their low excitation spectra (dotted line). The mobility edge is depicted as dashed line

a mobility edge in the samples A and B was observed. The energy position is indicated by a dashed line for both samples. In sample A a gain structure between 3.2 and 3.3 eV appears on the high-energy side of the amplified stimulated emission (ASE). For higher power densities a sharp structure centered around 3.22 eV strongly increases having a maximum gain value of 62 cm^{-1} . The onset of lasing in the structure is found at 1.2 MW/cm^2 . The correlation between optical gain and structural properties is again given in Table 1. We find that the MBE-grown sample A which exhibits a Gaussian CL histogram shows optical amplification at 7 K. In contrast, sample C (grown without MOVPE-GaN template) has a broad non-Gaussian luminescence distribution and shows no optical amplification. In sample B the lasing peak occurs in the centre of the gain structure, resulting in a low lasing threshold of about 600 kW/cm^2 at 300 K and high gain values up to 130 cm^{-1} at 6 K. From Table 1 one can see directly that there is a correlation of the σ – resembling mostly the degree of In fluctuations in the sample – and the observed gain values. The degree of In fluctuations, directly monitored by the CL histograms, determines the efficiency of optical amplification and therefore the gain and lasing threshold values of the samples. Since the onset of lasing and the optical gain are on the low energy side of the mobility edge in both samples we can conclude that localized carriers are responsible for the recombination and as efficient gain mechanism at least for lower temperatures. It is clear that the detrimental influence of strong piezoelectric fields in these samples reduces the recombination rate and optical amplification. This results in the suppression of optical gain and lasing in the MBE-grown sample A at 300 K.

Conclusions We have investigated the optical and structural properties of InGaN/GaN heterostructures grown by MBE and MOCVD using time-resolved PL, CL microscopy and gain spectroscopy. We provided evidence that localized carriers at potential fluctuations act as main recombination process and as gain mechanism at least at low temperatures. The recombination dynamics resulting in transients, which can be fitted by stretched exponential decays, the temperature dependent PL and CL measurements are explained with this model. Furthermore, it was evidenced that the degree of In fluctuations strongly influences the efficiency of the optical gain in all h-InGaN heterostructures. The growth temperature and the immiscibility of In in InGaN are influential coefficients to improve the reliability and performance of InGaN-based heterostructures.

References

- [1] S. NAKAMURA and G. FASOL, *The Blue Laser Diode*, Springer-Verlag, Berlin 1997.
- [2] Y.-H. KWON, G. H. GAINER, S. BIDNYK, Y.-H. CHO, J. J. SONG, M. HANSEN, and S. P. DENBAARS, *Appl. Phys. Lett.* **75**, 2545 (1999).
- [3] T. WANG, D. NAKAGAWA, M. LACHAB, T. SUGAHARA, and S. SAKAI, *Appl. Phys. Lett.* **74**, 3128 (1999).
- [4] H. KOLLMER, J. S. IM, S. HEPPLE, J. OFF, F. SCHOLZ, and A. HANGLEITER, *Appl. Phys. Lett.* **74**, 82 (1999).
- [5] I.-H. HO and G. B. STRINGFELLOW, *Appl. Phys. Lett.* **69**, 2701 (1996).
- [6] K. P. O'DONNELL, R. W. MARTIN, and P. G. MIDDLETON, *Phys. Rev. Lett.* **82**, 237 (1999).
- [7] J. DALFORS, J. P. BERGMAN, P. O. HOLTZ, B. E. SERNELIUS, B. MONEMAR, H. AMANO, and I. AKASAKI, *Appl. Phys. Lett.* **74**, 3299 (1999).
- [8] J. S. IM, H. KOLLMER, J. OFF, A. SOHMER, F. SCHOLZ, and A. HANGLEITER, *Phys. Rev. B* **57**, R9435 (1998).
- [9] F. BERTRAM, T. RIEMANN, J. CHRISTEN, A. KASCHNER, A. HOFFMANN, C. THOMSEN, K. HIRAMATSU, T. SHIBATA, and N. SAWAKI, *Appl. Phys. Lett.* **74**, 359 (1999).
- [10] K. L. SHAKLEE, R. E. NAHORY, and R. F. LEHENY, *J. Lumin.* **7**, 284 (1973).
- [11] T. RIEMANN, D. RUDLOFF, J. CHRISTEN, A. KROST, M. LÜNENBURGER, H. PROTZMANN, and M. HEUKEN, *phys. stat. sol. (b)* **216**, 301 (1999).
- [12] Y.-H. CHO, G. H. GAINER, A. J. FISCHER, J. J. SONG, S. KELLER, U. K. MISHRA, and S. P. DENBAARS, *Appl. Phys. Lett.* **73**, 1370 (1998).
- [13] X. ZHANG, D. H. RICH, J. T. KOBAYASHI, N. P. KOBAYASHI, and P. D. DAPKUS, *Appl. Phys. Lett.* **73**, 1430 (1998).
- [14] M. POPHRISTIC, F. H. LONG, C. TRAN, R. F. KARLICEK, Z. C. FENG, and I. T. FERGUSON, *Appl. Phys. Lett.* **73**, 815 (1998).